

Fishtail effect studied by ac susceptibility in $\text{ErBa}_2\text{Cu}_3\text{O}_{7-\delta}$ single crystal

C. A. Cardoso

Departamento de Física, UFSCar, Caixa Postal 676, 13565-905, São Carlos-São-Paulo, Brazil

O. F. de Lima

Instituto de Física "Gleb Wataghin," UNICAMP, 13083-970, Campinas-São-Paulo, Brazil

(Received 9 July 2003; accepted 30 October 2003)

The second magnetization peak (SMP), also known as the fishtail effect, is studied by a scaling procedure for ac susceptibility measurements. From this scaling law the frequency dependence of the critical current $J(\nu)$ and the flux creep exponent n can be determined. A striking correlation between n and the SMP is observed, which indicates a clear change in the rate of flux creep around the peak position. This result points to the relevance of the dynamical contribution for the peak formation. However, we could not observe a transition between two different regimes of vortex motion at the SMP. The dependence of the SMP with sample dimensions is also discussed. © 2004 American Institute of Physics. [DOI: 10.1063/1.1636261]

I. INTRODUCTION

One of the numerous properties of superconductors that has its interest revived with the discovery of high- T_c superconductors is the so-called *fishtail effect*, also known as *peak effect* or *second magnetization peak* (SMP), which corresponds to an anomalous increase on the width ΔM of the magnetic hysteresis loop. Although such phenomenon was observed in conventional superconductors several years ago,¹ and in high- T_c more recently,² its origin is still controversial. Since ΔM is proportional to the critical current density,³ several authors proposed that an increase in the efficiency of pinning centers with increasing magnetic fields could lead to the appearance of the second magnetization peak.^{2,4,5} This was emphasized by fast magnetization measurements using pulsed field and vibrating sample magnetometer measurements,⁶ which revealed the SMP even at very short time windows. Such nonmonotonic dependence of the critical current with the applied field could be of great technological interest, since it could be used to improve the performance of superconducting devices. However, as pointed by some other authors, it is possible that different dynamical processes could also lead to the appearance of the fishtail effect. It is well known that high- T_c superconductors present very intense magnetic relaxation,⁷ therefore the occurrence of strong vortex creep should be considered in the analysis of magnetization data in these materials. Transitions between different flux creep regimes,⁸⁻¹⁰ or from elastic to plastic flow,^{11,12} introduce changes in the magnetic relaxation rates, and therefore can produce hysteresis loops with widths that do not decrease monotonically with an increase of the applied magnetic field. More recently, the possibility of an order-disorder transition leading to the appearance of the SMP was addressed both theoretically¹³ and experimentally.¹⁴ A less explored characteristic of the SMP is its dependence with sample dimensions. Besides the geometric factors associated with demagnetization fields, sample size can eventually play a significant role in the development of the fishtail effect. For instance, the occurrence of vortex

avalanches could lead to different average relaxation rates and thus to SMP formation.^{15,16} Those flux-jump instabilities are present when the local temperature increases due to the energy dissipated during flux jumps. If the magnetic diffusion time is much shorter than the thermal diffusion time, an adiabatic heating occurs locally in the sample, leading to catastrophic vortex avalanches. Once the local heating depends on sample heat exchange with the environment, which depends on sample dimensions, the development of a SMP will depend on sample dimensions too. Actually, this model predicts a critical dimension below which there are no more flux-jump instabilities and the SMP should disappear. Furthermore, models that consider inhomogeneities as the key factor to the development of the SMP may also explain its size dependence. Indeed, some authors¹⁷ have explored how weak macroscopic inhomogeneities can affect the electromagnetic properties of a superconducting sample, including the appearance of a SMP. The importance of inhomogeneities for the development of the SMP has also been observed experimentally.^{18,19}

In this work we present a study of the SMP using a scaling procedure for ac susceptibility measurements, in an $\text{ErBa}_2\text{Cu}_3\text{O}_{7-\delta}$ single crystal, and explore its sample size dependence. ac susceptibility (χ) is a very versatile technique, widely used in the study and characterization of superconducting materials.²⁰ Its major advantages are the experimental simplicity, low cost, and great sensitivity. However, quantitative analysis of ac susceptibility data until recently have been somewhat limited and not reliable, due to the lack of a theory that considers the actual sample and field geometries occurring in each experiment. Only geometries where demagnetizing effects could be neglected, like an infinite cylinder²¹ or a slab²² in parallel applied field, were considered for a long time. This situation has been considerably improved after the formulation of a theory^{23,24} that gives precise results, including flux creep effects, for several finite sample geometries. An interesting result derived in these works is the formulation of a scaling law for ac susceptibility measurements, relating amplitude (h) and frequency (ν) of

the excitation field. This scaling law for $\chi(h, \nu)$ has been extended^{25–27} to provide information about the critical current density and the relaxation process directly from ac susceptibility measurements. In fact, it was shown²⁵ that the nonlinear complex susceptibility is a function of the scaling variable $\tilde{h} = hJ(\nu_{\text{ref}})/J(\nu)$, where J is the induced current density, and ν_{ref} is an arbitrary reference frequency. By measuring a set of $\chi(h, \nu)$ curves at different frequencies ν and amplitudes h , it is possible to extract the frequency dependent $J(\nu)$. Thus, this simple scaling procedure could be used to study the dynamical processes occurring in the sample, in time windows very different from those usually accessed by slow magnetic relaxation measurements. One major limitation of this approach is that it applies only for strongly nonlinear magnetic response, corresponding to a temperature interval near T_c where intense flux motion occurs. Although this limitation is not specially severe for high- T_c superconductors, it presents a more serious constraint to the study of conventional, low T_c , materials.

II. SAMPLE AND EXPERIMENTAL DETAILS

The sample employed in this work was a high quality $\text{ErBa}_2\text{Cu}_3\text{O}_{7-\delta}$ single crystal, having dimensions $1.4 \times 0.3 \times 0.01 \text{ mm}^3$, grown by the traditional self-flux method in an yttria-stabilized zirconia crucible. The sample presents a superconducting transition temperature $T_c = 90 \text{ K}$.

All ac susceptibility measurements were performed in a commercial physical properties measurement system (PPMS) made by Quantum Design Company. Several sets of χ measurements were taken as a function of $h(0.1–17 \text{ Oe})$ for fixed frequencies ν from 10 Hz to 10 kHz. The data were normalized such that $\chi(h, \nu) = -1$ when $h \rightarrow 0.1$, corresponding to the constant region for lower values of h in the $\chi \times h$ curves. Before taking each $\chi \times h$ curve a constant magnetic field $H_a \gg H_{c1}(T^*)$ was applied to the sample in the normal state (H_{c1} is the lower critical field). Following, the sample was then cooled down to the measuring temperature T^* . This procedure aimed at establishing a fully penetrated flux distribution in the entire sample. The $M \times H$ loops were measured in a superconducting quantum interference device (SQUID) magnetometer MPMS-5, also made by Quantum Design.

III. RESULTS AND DISCUSSION

Figure 1 shows $M \times H$ curves for two different temperatures, 70 and 80 K, both presenting a large SMP. The SMP position, H_{SMP} , was found to be 11 kOe at $T = 70 \text{ K}$, and 5 kOe at $T = 80 \text{ K}$. In fact, a systematic shift of the SMP towards higher fields is observed as the temperature is decreased. As shown in Fig. 2, H_{SMP} presents a linear dependence with temperature, with $S \equiv \partial H_{\text{SMP}} / \partial T = -0.62 \text{ kOe/K}$. This slope is much smaller than most reported values of $S = 7–100 \text{ kOe/K}$ for YBCO crystals,^{28,29} being close to (but still smaller than) the value of $S = 1.7 \text{ kOe/K}$, obtained by Klein *et al.*³⁰ also for YBCO crystals, and $S \sim 1 \text{ kOe/K}$ obtained by Mochida and Murakami for Nd123 crystals.³¹

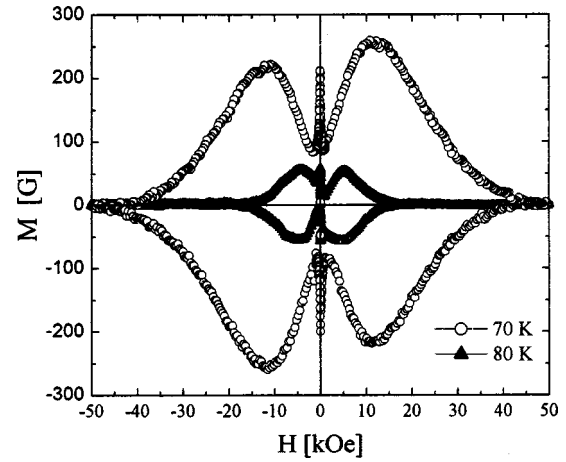


FIG. 1. Hysteresis loops for $T = 80$ and 70 K , showing a clear SMP.

To study the SMP using the amplitude-frequency scaling law,²⁵ we have plotted the $\chi(h, \nu)$ data against the scaling variable $\tilde{h} = h[J(500)/J(\nu)]$. Here, $J(500)$ is a normalizing shielding current for the reference frequency $\nu_{\text{ref}} = 500 \text{ Hz}$. The practical fitting operation consists of finding the appropriate multiplicative factor $J(500)/J(\nu)$ that transforms the horizontal scale h of each measured curve $\chi'(h, \nu)$, in order to superimpose it with the reference curve $\chi'(h, 500 \text{ Hz})$. In all cases the imaginary component $\chi''(h, \nu)$ is expected to collapse automatically into a single universal curve for the best fitted factor $J(500)/J(\nu)$, obtained from the scaling of the real part of the complex susceptibility. By this procedure the frequency dependence of the induced current density $J(\nu)$ can be determined and compared with available models. Therefore, this procedure allows the direct determination of the most suitable model for the vortex dynamics, instead of assuming *a priori* a specific theory to model the experimental data. More details about this procedure can be found in Ref. 26.

Figures 3, 4, and 5 show double logarithmic plots of $\chi(h, \nu)$ as a function of \tilde{h} for three dc fields and temperature of 80 K. These measurements were taken at magnetic fields below, above and at H_{SMP} . For the sake of brevity only

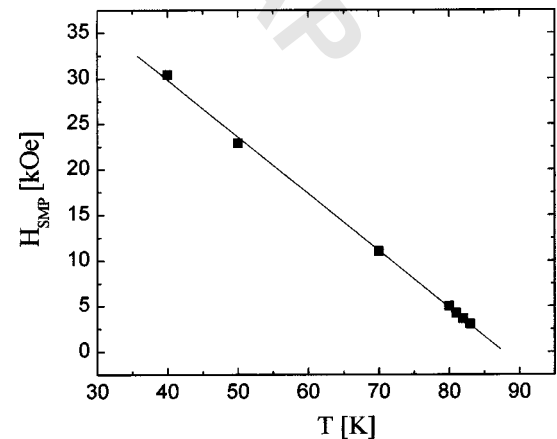


FIG. 2. Second magnetization peak position as a function of temperature. The solid line is the best linear fitting.

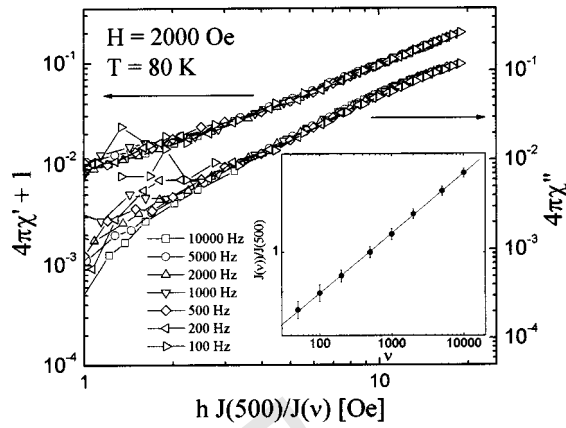


FIG. 3. Complex susceptibility as a function of the scaled amplitude, for $H=2$ kOe and $T=80$ K. The inset shows the frequency dependent current density obtained from the scaling procedure. The current density follows a power law as predicted by the collective creep/vortex glass models.

results for $T=80$ K are presented, since the results found for 70 K were similar. In order to span the vertical scale (left axis) close to $4\pi\chi' = -1$ we have used the more convenient variable $4\pi\chi' + 1$. We found a very good collapse of all curves for different frequencies in a single universal curve for χ' . The scaling of the imaginary component χ'' is also quite good at higher amplitudes, but a deterioration of the signal-to-noise ratio at low amplitudes is observed.

The insets of Figs. 3–5 show plots of the obtained frequency dependence for the normalized current density $J(\nu)/J(500)$ in the corresponding fields and $T=80$ K. The solid lines represent excellent linear fits to the experimental points. For all magnetic fields and temperatures tested, including $T=70$ K (not shown), $J(\nu)$ followed a power law dependence with frequency which can be described by the formula^{25,32,33}

$$J(\nu, T, H) = J_c(T, H) \left(\frac{\nu}{\nu_0} \right)^{1/n}, \quad (1)$$

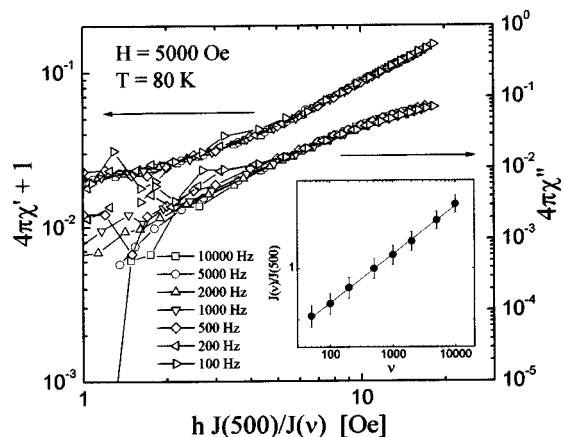


FIG. 4. Complex susceptibility as a function of the scaled amplitude, for $H=5$ kOe and $T=80$ K. The inset shows the frequency dependent current density obtained from the scaling procedure. The current density follows a power law as predicted by the collective creep/vortex glass models.

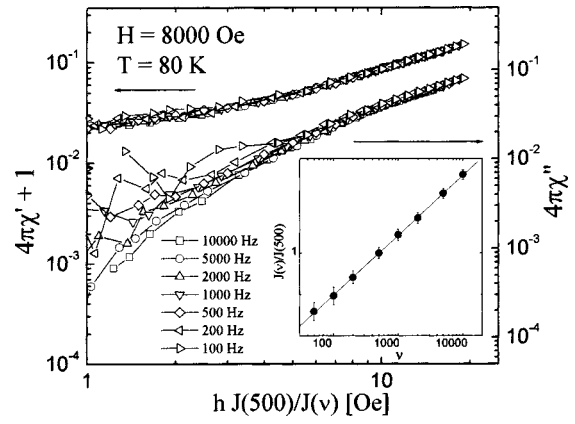


FIG. 5. Complex susceptibility as a function of the scaled amplitude, for $H=8$ kOe and $T=80$ K. The inset shows the frequency dependent current density obtained from the scaling procedure. The current density follows a power law as predicted by the collective creep/vortex glass models.

where J_c is the critical current density, $n = U_c(T, H)/kT$ is the creep exponent, $U_c(T, H)$ is an activation energy, k is the Boltzmann constant, and ν_0 is a normalizing frequency interpreted as an intrinsic attempt frequency of vortex jumps.^{32,34} Equation (1) was derived from a more general expression $J(\nu, T, H) = J_c(T, H) g[kT \ln(\nu/\nu_0)/U]$ that incorporates the frequency dependence. The function $0 < g\{y\} < 1$ describes the effective reduction of the critical current density during one period of the ac field, and depends on the regime of thermally activated flux motion. In the so-called logarithmic approximation,³⁵ $U = U_c(T, H) \ln(J_c/J)$, the collective flux creep theory predicts⁸ $g\{y\} = \exp(-y)$, thus leading to Eq. (1).

According to Eq. (1) the slopes of the fitted straight lines in the insets of Figs. 3–5 give $1/n$. The creep exponent n indicates the relevance of flux creep,²³ such that a smaller value of n corresponds to a higher creep rate and vice-versa. Therefore, by probing the magnetic field dependence of n , it is possible to identify changes in vortex motion for different applied magnetic fields. Once different creep rates are observed for $H \approx H_{\text{SMP}}$ and considering the relatively long measuring time of the SQUID magnetometer, we could safely conclude that a dynamical contribution to the SMP (Fig. 1) is present. In fact, as shown in Fig. 6, a remarkable correlation between the SMP and the peak position of the creep exponent n was found. For both temperatures, n presents a maximum around H_{SMP} (see also Fig. 1). The solid lines were obtained from the interpolation formula¹⁷

$$n(H) = 1 + \left[s_{\text{SMP}}^2 + s_1^2 \left(\frac{H}{H_{\text{SMP}}} - 1 \right)^2 \right]^{-1/2}, \quad (2)$$

where $s_{\text{SMP}} = 1/(n_{\text{SMP}} - 1)$ and $s_1 = s_1(T)$ is a fitting parameter. This behavior indicates a relevant reduction in the vortices relaxation rate at magnetic fields around H_{SMP} . Actually, as shown in the inset of Fig. 6, if one plots the creep exponent normalized by its maximum value as a function of the normalized field H/H_{SMP} the curves obtained for both temperatures basically become coincident. There is no indication of a transition, at H_{SMP} , from a regime of fast relaxation to another one, with a smaller relaxation rate.^{8–10} The

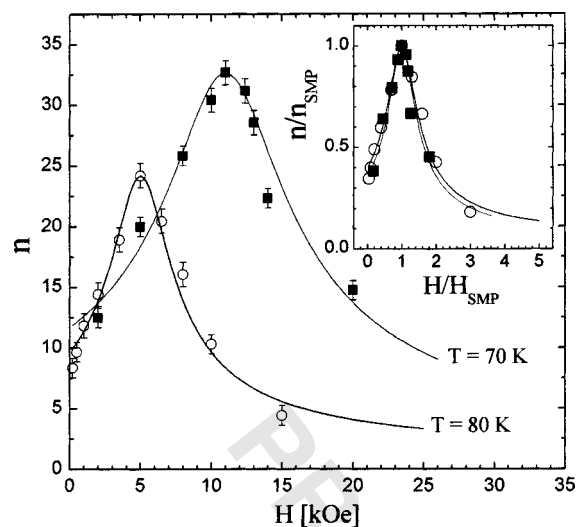


FIG. 6. Creep exponent for both temperatures 70 and 80 K. Inset presents the normalized creep exponent in terms of the normalized field. The solid lines correspond to the best fitting of Eq. (2).

frequency dependence of $J(\nu)$ as given by Eq. (1) does not change at H_{SMP} , indicating also that the same pinning mechanism is effective above and below the peak position. Although these results unequivocally point to a dynamical contribution to the SMP, they do not rule out a possible enhancement of pinning efficiency at $H \sim H_{SMP}$. Such change in the pinning strength, by applying a field $H \sim H_{SMP}$, would also lead to a reduction in the magnetic relaxation rate.

IV. SIZE EFFECTS IN THE SECOND MAGNETIZATION PEAK

In order to obtain additional information about the possible origins of the fishtail effect, we have studied its dependence with sample size. The crystal employed in the first part of this work was carefully cleaved in pieces of average dimensions $0.17 \times 0.25 \times 0.01 \text{ mm}^3$, as shown in Fig. 7. The entire set of measurements done to the whole sample was then repeated.

In Fig. 8 we present the hysteresis loops, for both temperatures of 70 and 80 K, obtained before (open symbols) and after (solid symbols) cleaving the sample. It can be observed that the SMP position shifts to lower fields in both cases and the SMP is partially suppressed. This should be contrasted with a previous work on Tl based superconductors which did not show any change in the SMP position with sample size reduction, although the suppression of the SMP was verified.³⁶ The reduction rate of H_{SMP} with increasing temperature, given by $\partial H_{SMP} / \partial T$, does not present any significant change for the cleaved the sample, remaining around 0.6 kOe/K. This fact seems to indicate that the mechanism responsible for the SMP formation remains qualitatively the same after cleaving the sample.

Using the same scaling procedure for ac susceptibility measurements as done before, we found again an excellent superposition of all curves for different frequencies (not shown). The values obtained for the creep exponent in the cleaved sample, at 80 K, are presented in Fig. 9. The maxi-

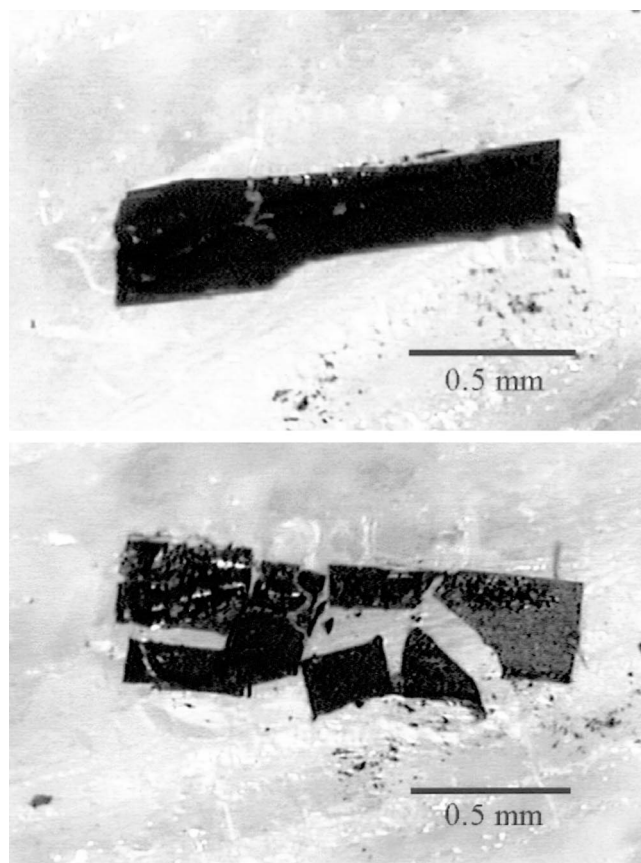


FIG. 7. Pictures of the original sample (top) and after it was cleaved (bottom). The clear regions on top and around the sample are residues of silicone grease.

um position shifts to lower magnetic fields, following the change in the second magnetization peak observed in the hysteresis loops, thus reinforcing the correlation between the creep exponent n and the occurrence of the SMP. The solid lines were obtained from Eq. (2). One can observe an overall reduction of n after cleaving the sample, for $H \geq H_{SMP}$, while for $H < H_{SMP}$ it is observed a slight increase in n values. The maximum value for the creep exponent, n_{SMP} , is smaller for the cleaved sample, indicating that in this situation there is an increase in vortex motion around H_{SMP} . In fact, the creep exponent presents a weaker magnetic field dependence for the cleaved sample, implying smaller changes in the magnetic relaxation rate at different magnetic fields. Assuming that magnetic relaxation is the most important factor for the SMP appearance, smaller changes in the creep rate leads to less prominent SMP. Therefore, the results obtained for n presented in Fig. 9 are consistent with the reduction of the SMP observed in Fig. 8. It is interesting to compare the increase in the creep exponent due to changes in temperature and by reducing the sample dimensions. As shown in Fig. 6, the influence of the increase in temperature on n may be described basically as a shift in the peak position to a lower magnetic field and an overall reduction in its values, consistent with the expected increase in the creep rate at higher temperatures. The measurements presented in Fig. 9, on the other hand, were performed at the same temperature. Therefore, thermal activation could not be responsible

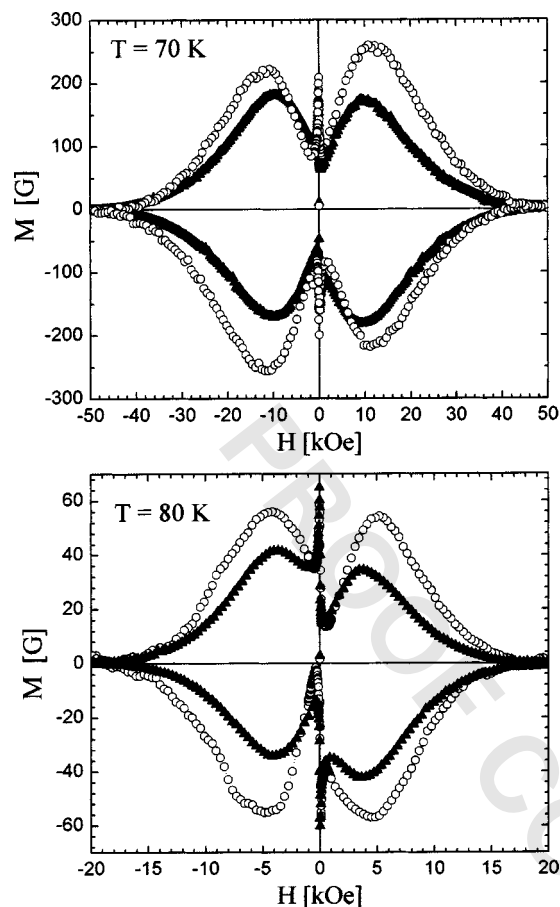


FIG. 8. Comparison of hysteresis loops measured before (open symbols) and after (solid symbols) cleaving the sample, for temperatures (a) 70 and (b) 80 K.

for the changes in the creep exponent observed in Fig. 9. The difference between the SMP reduction, by warming the sample or by cleaving it, can be emphasized by the normalized plots shown in the insets of Figs. 6 and 9. Here we

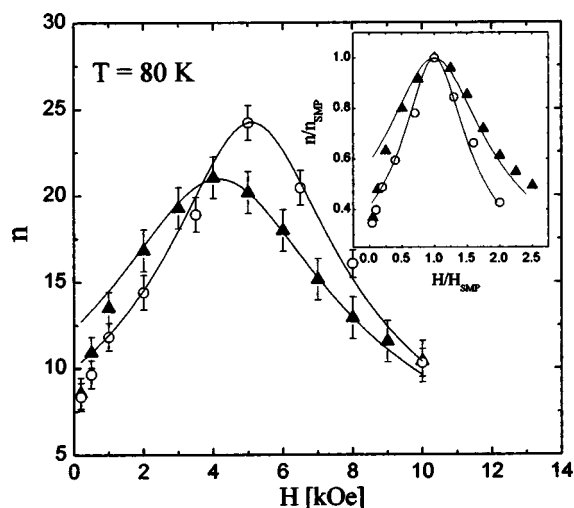


FIG. 9. Comparison of the creep exponent values obtained before (open symbols) and after (solid symbols) cleaving the sample, for $T=80$ K. The inset presents the normalized creep exponent for both sample conditions and $T=80$ K. The solid lines correspond to the best fitting of Eq. (2).

observe that the normalized curves change significantly with cleaving the sample (inset of Fig. 9), while they remain almost the same with the change in temperature for a given sample (inset of Fig. 6).

These results indicate that the mechanism responsible for the development of the SMP in this sample is sensitive to extrinsic factors like sample dimensions. One possible explanation for this dependence comes from the influence of sample inhomogeneities that could affect its global magnetic properties. It is known³⁷ that the local current density in high-temperature superconductors present significant spatial variations over macroscopic scales $L \sim 1 \mu\text{m} - 1 \text{mm}$. These perturbations come from weak inhomogeneities of the sample, always observed even in the best crystals. One important consequence of these inhomogeneities is that the mean current density \bar{J} , which is calculated by the statistical average of the local current density, may present complex dependencies with temperature and electric and magnetic fields.¹⁷ In particular, a nonmonotonic dependence of \bar{J} with the magnetic field may occur, producing a SMP. Since different regions of the sample present different dependencies with the local magnetic and electric fields, by cleaving the sample it is possible to affect \bar{J} and its dependence with the local magnetic field, consequently affecting the SMP. Therefore, the observed dependence of the SMP with sample dimensions may indicate that inhomogeneities could be the cause of the appearance of the SMP in our sample.

V. CONCLUDING REMARKS

In this work we presented experimental results that support (a) a dynamical contribution to the development of the SMP and (b) a dependence of the SMP with sample size. To reach such conclusions we have applied an analysis based on a scaling law for ac susceptibility measurements, which allowed us to directly observe the frequency dependence of $J(\nu)$ and obtain the vortex creep exponent n . The critical current presented a power law dependence with frequency at all temperatures, applied magnetic fields, and sample dimensions tested. The creep exponent presented a maximum at H_{SMP} , following the SMP shift with changes in temperature or sample size. Although our results point to the relevance of dynamical effects in the development of the fishtail effect, we did not observe a clear transition in vortex dynamics at H_{SMP} , which could correspond to two different regimes, one above and another below the peak position. Instead, we concluded that the appearance of the SMP in our sample is intrinsically related with the presence of weak inhomogeneities in our Er-123 crystal. Such inhomogeneities affect the mean current density \bar{J} within the sample, making possible its nonmonotonic dependence with the local magnetic field, which can cause the appearance of the SMP.

ACKNOWLEDGMENTS

The authors are thankful to M. A. Avila and R. A. Ribeiro for helping in the preparation of the Er-123 crystal studied in this work. They also acknowledge Y. Kopelevich for stimulating discussions. This work was supported by Bra-

zilian agencies Fundação de Amparo a Pesquisa do Estado de São Paulo (FAPESP) and Conselho Nacional de Pesquisas (CNPq).

- ¹T. G. Berlincourt, R. R. Hake, and D. H. Leslie, *Phys. Rev. Lett.* **6**, 671 (1961).
- ²M. Däumling, J. M. Seuntjens, and D. C. Larbalestier, *Nature (London)* **346**, 332 (1990).
- ³C. P. Bean, *Phys. Rev. Lett.* **8**, 250 (1962); *Rev. Mod. Phys.* **36**, 31 (1964).
- ⁴J. L. Vargas and D. C. Larbalestier, *Appl. Phys. Lett.* **60**, 1741 (1992).
- ⁵M. S. Osofsky, J. L. Cohn, E. F. Skelton, M. M. Miller, R. J. Soulen, Jr., S. A. Wolf, and T. A. Vanderah, *Phys. Rev. B* **45**, 4916 (1992).
- ⁶W. Harneit *et al.*, *Physica C* **267**, 270 (1996).
- ⁷Y. Yeshurun, A. P. Malozemoff, and A. Shaulov, *Rev. Mod. Phys.* **68**, 911 (1996).
- ⁸G. Blatter, M. V. Feigel'man, V. B. Geshkenbein, A. I. Larkin, and V. M. Vinokur, *Rev. Mod. Phys.* **66**, 1125 (1994).
- ⁹L. Krusin-Elbaum, L. Civale, V. M. Vinokur, and F. Holtzberg, *Phys. Rev. Lett.* **69**, 2280 (1992).
- ¹⁰Y. Yeshurun, N. Bontemps, L. Burlachkov, and A. Kapitulnik, *Phys. Rev. B* **49**, 1548 (1994).
- ¹¹Y. Abulafia *et al.*, *Phys. Rev. Lett.* **77**, 1596 (1996).
- ¹²J. W. Farmer, M. Kornecki, and D. L. Cowan, *Physica C* **364**, 334 (2001).
- ¹³G. P. Mikitik and E. H. Brandt, *Phys. Rev. B* **64**, 184514 (2001).
- ¹⁴Y. Yamaguchi, N. Shirakawa, G. Rajaram, K. Oka, A. Mumtaz, H. Obara, T. Nakagawa, and H. Bando, *Physica C* **361**, 244 (2001).
- ¹⁵Y. Kopelevich and P. Esquinazi, *J. Low Temp. Phys.* **113**, 1 (1998).
- ¹⁶P. Esquinazi, A. Setzer, D. Fuchs, Y. Kopelevich, E. Zeldov, and C. Assmann, *Phys. Rev. B* **60**, 12454 (1999).
- ¹⁷A. Gurevich and V. M. Vinokur, *Phys. Rev. Lett.* **83**, 3037 (1999).
- ¹⁸X. Y. Cai, A. Gurevich, D. C. Larbalestier, R. J. Kelley, M. Onellion, H. Berger, and G. Margaritondo, *Phys. Rev. B* **50**, 16774 (1994).
- ¹⁹W. A. C. Passos, P. N. Lisboa-Filho, R. Caparroz, C. C. de Faria, P. C. Venturini, F. M. Araujo-Moreira, S. Sergeenkov, and W. A. Ortiz, *Physica C* **354**, 189 (2001).
- ²⁰See, e.g., *Magnetic Susceptibility of Superconductors and Other Spin Systems*, edited by R. A. Hein, T. L. Francavilla, D. H. Liebenberg (Plenum, New York, 1991).
- ²¹J. R. Clem, H. R. Kerchner, and S. T. Sekula, *Phys. Rev. B* **14**, 1893 (1976).
- ²²L. Ji, H. R. Sohn, G. C. Spalding, C. J. Lobb, and M. Tinkham, *Phys. Rev. B* **40**, 10936 (1989).
- ²³E. H. Brandt, *Phys. Rev. B* **58**, 6506 (1998).
- ²⁴E. H. Brandt, *Phys. Rev. B* **58**, 6523 (1998).
- ²⁵O. F. de Lima and C. A. Cardoso, *Phys. Rev. B* **61**, 11722 (2000).
- ²⁶C. A. Cardoso and O. F. de Lima, *Physica C* **334**, 185 (2000).
- ²⁷C. A. Cardoso, M. A. Avila, R. A. Ribeiro, and O. F. de Lima, *Physica C* **354**, 165 (2001).
- ²⁸T. K. Worthington, W. J. Gallagher, and T. R. Dinger, *Phys. Rev. Lett.* **59**, 1160 (1987).
- ²⁹U. Welp, S. Fleshler, W. K. Kwok, R. A. Klemm, V. M. Vinokur, J. Downey, B. Veal, and G. W. Crabtree, *Phys. Rev. Lett.* **67**, 3180 (1991).
- ³⁰L. Klein, E. R. Yacoby, Y. Yeshurun, A. Erb, G. Müller-Vogt, V. Breit, and H. Wühl, *Phys. Rev. B* **49**, 4403 (1994).
- ³¹T. Mochida and M. Murakami, *Physica C* **290**, 311 (1997).
- ³²L. Fàbrega, J. Fontcuberta, L. Civale, and S. Piñol, *Phys. Rev. B* **50**, 1199 (1994).
- ³³B. J. Jönsson, K. V. Rao, S. H. Yun, and U. O. Karlsson, *Phys. Rev. B* **58**, 5862 (1998).
- ³⁴L. Fàbrega, J. Fontcuberta, S. Piñol, C. J. van der Beek, and P. H. Kes, *Phys. Rev. B* **47**, 15250 (1993).
- ³⁵E. Zeldov, N. M. Amer, G. Koren, A. Gupta, M. W. McElfresh, and R. J. Gambino, *Appl. Phys. Lett.* **56**, 680 (1990).
- ³⁶V. Hardy, A. Wahl, A. Ruyter, A. Maignan, C. Martin, L. Coudrier, J. Provost, and Ch. Simon, *Physica C* **232**, 347 (1994).
- ³⁷A. E. Pashitski *et al.*, *Science* **275**, 367 (1997).